EasyChair Preprint

№ 1552

Docking simulation of Chemerin-9 and ChemR23 receptor

Keiichi Nobuoka, Hironao Yamada, Takeshi Miyakawa,
Ryota Morikawa, Takuya Watanabe and Masako Takasu

September 23, 2019

Docking simulation of Chemerin-9 and ChemR23 receptor

Keiichi Nobuoka
Computational Biophysics Laboratory in Tokyo University of Pharmacy and Life Sciences
Tokyo, Japan
+81-42-676-8920
s149093@toyaku.ac.jp

Hironao Yamada
Computational Biophysics Laboratory in Tokyo University of Pharmacy and Life Sciences, Pharmacy
Tokyo, Japan
hyamada@toyaku.ac.jp

Takeshi Miyakawa
Computational Biophysics Laboratory in Tokyo University of Pharmacy and Life Sciences
Tokyo, Japan
takeshi@toyaku.ac.jp

Ryota Morikawa
Computational Biophysics Laboratory in Tokyo University of Pharmacy and Life Sciences
Tokyo, Japan
morikawa@toyaku.ac.jp

Takuya Watanabe
Laboratory of Cardiovascular Medicine in Tokyo University of Pharmacy and Life Sciences
Tokyo, Japan
watanabe@toyaku.ac.jp

Masako Takasu
Computational Biophysics Laboratory in Tokyo University of Pharmacy and Life Sciences
Tokyo, Japan
takasu@toyaku.ac.jp

ABSTRACT

Chemerin-9 is a nonapeptide that corresponds to the YFPGQFAFS sequence on the C-terminal side of Chemerin protein. In recent years, in clinical studies and animal studies using mice, it has been reported that Chemerin-9 binds to the ChemR23 receptor and can suppress the inflammation-related diseases such as arteriosclerosis.

In this study, molecular dynamics simulations were performed with the Chemerin-9 peptide to identify structures with high and low free energy. Docking simulations of these structures of Chemerin-9 and ChemR23 receptor were performed, and the docking model with the lowest free energy and binding energy of Chemerin was identified. For this model, the evaluation of binding sites and binding forces is performed. Based on these findings, we will aim to give insights to the development of new drugs that suppress arteriosclerosis.

Keywords

Atherosclerosis; Chemerin-9; ChemR23; ligand; receptor; molecular dynamics simulations; docking simulations; hydrogen bonds

1. INTRODUCTION

Arteriosclerosis, also called atherosclerosis, forms a plaque by the accumulation of lipids such as cholesterol and cholesterol ester called atheromas in the intima of medium-and large-sized arteries including coronary, cerebral, and carotid arteries and aorta, which narrows the lumen of blood vessels [1]. Furthermore, the plaque can also rupture easily, leading to thrombosis and sudden occlusion of blood vessels [1].

In the experiments by Sato, K. et al. [2], the suppressive effects of Chemerin on aortic atherosclerosis in apolipoprotein E-deficient mice (in vivo), THP-1 monocyte adhesion to human umbilical vein endothelial cells (HUVECs), and the foaming of THP-1 monocyte-derived macrophages (in vitro) were reported. This study was conducted to evaluate the effect of Chemerin on atheroprotective effects in HUVECs and human aortic smooth muscle cells (HASMC). As a result, in vivo, in mice receiving Chemerin, the formation of foam cells causing atherosclerosis was suppressed, and the progression of atherosclerotic lesions of the aorta was prevented. In vitro, Chemerin also inhibited monocyte adhesion to HUVECs, suppressed oxidized low-density lipoprotein-induced foam cell formation in THP-1 monocyte-derived macrophages, and suppressed the migration and proliferation of HASMC. In addition, even when the peptide was changed to Chemerin-9, the result of inhibiting atherosclerosis was obtained. From these facts, the part of Chemerin called Chemerin-9 is active.

Chemerin is also known as tazarotene-induced gene 2 (TIG2), retinoic acid receptor responder 2 (RARRES2), or RAR-responsive protein TIG2, and in human's protein information is encoded on chromosome 7 [3]. When transcribed and translated, it is produced as a protein composed of 163 amino acids. The protein in this state is also called preprochemerin. For this protein to be active, the N-terminal signal peptide (1st to 20th amino acids) and the C-terminal peptide (158th to 163rd) must be cleaved [4]. In addition, studies have shown that the part of the peptide composed of amino acids 149 to 157 of Chemerin, called Chemerin9 in this protein, is the active site [5]. In particular, it has been reported that the first residue Y, the second residue F, the fourth residue G, the sixth residue F, and the eighth residue F of Chemerin 9 are important for activity [6]. Studies have also reported that Chemerin must bind to the ChemR23 receptor for activity [7, 8].

ChemR23 receptor is a protein encoded by Chemokine likd receptor 1 (CMKLR1) gene [9], and is a G protein receptor composed of 371 amino acids. This receptor expected to bind Chemerin and Chemerin-9. Upon binding, the receptor is activated, recruits intracellular calcium and triggers activation of several other signaling cascades such as extracellular signal-regulated protein kinase 1/2 and nuclear factor-κB. This plays a major role in suppressing the inflammation-related diseases such as atherosclerosis.

In this study, we investigated the structures and dynamics of the chemerin-9 by performing molecular dynamics (MD) simulations to study structural stability. Next, we simulated docking with chemerin-9 and ChemR23 receptor. Then, we compare bond strength of these models by affinity and hydrogen bonds.

2. MODELS and METHODS

2.1 Molecular Models

Since the structure of chemerin is not registered in the Protein Data Bank, a molecular model was created on a structure prediction site called I-TASSER [10] based on amino acid residues. A portion corresponding to Chemerin-9 was extracted from the created Chemerin molecular model and used as a Chemerin-9 molecular model. The structure of ChemR23 is also not registered in the Protein Data Bank. Therefore, a molecular model was created from the structure prediction as in Chemerin (Figure 1).

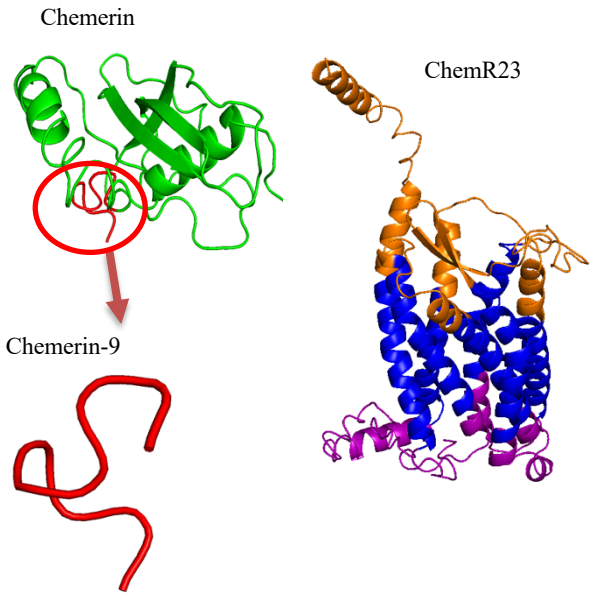

Figure 1. Molecular models of Chemerin, ChemR23, and Chemerin-9. In figure of ChemR23, orange is extracellular area, blue is cell membrane area, and purple is cytoplasmic area.

2.2 Molecular Dynamics Simulation

Molecular dynamics simulation was performed for Chemerin-9 with software Gromacs 2016.3 [11]. The box size was 3.88 nm x 3.88 nm x 3.88 nm with periodic boundary condition. Solvent was water molecules (SPC/E) 1672 [12], and force field was AMBER99 SB-ILDN [13].

2.3 Docking Simulation

Docking simulations of Chemerin-9 and ChemR23 were performed. Six structures of Chemerin-9 were extracted from the free energy topography obtained from the simulation described in the previous section. Each structure was docked with molecular model of ChemR23. AutoDock Vina [14] was used for this simulation.

3. RESULTS

3.1 Molecular Dynamics Simulation

With the result of molecular dynamics simulation, analysis was performed using RMSD, Rg, RMSF, and free energy landscape.

3.1.1 RMSD

RMSD is root mean square displacement, which is a physical quantity representing a shift between the reference structure and the structure at a certain time.

$$RMSD(t_1, t_2) = \sqrt{\frac{1}{M}\sum_{i=1}^{N} m_i\{\boldsymbol{r}_i(t_1) - \boldsymbol{r}_i(t_2)\}^2}$$

M is total mass, N is the total number of particles, t_1, t_2 is time, m_i is mass of atom i, and $\boldsymbol{r}_i$ is the position of atom i.

Here, RMSD for backbone was used. The result is shown in Figure 2. Immediately after starting the simulation, it changed from 0.25 to 0.4, and this continued until 300 ns.

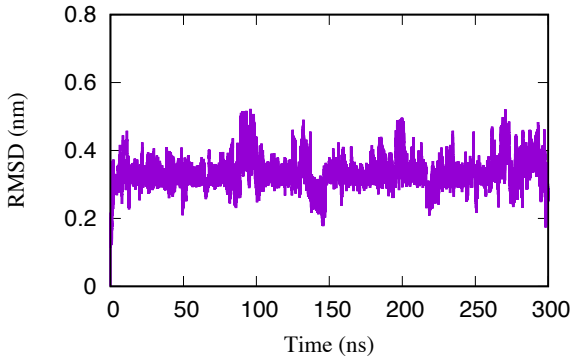

Figure 2. RMSD for chemerin-9.

3.1.2 R_g

R_g is the radius of gyration and is a physical quantity that represents the spread of the structure from the center of gravity of the protein molecule.

$$R_g = \sqrt{\frac{1}{M}\sum_{i=1}^{N} m_i(\boldsymbol{r}_i - \boldsymbol{r}_G)^2}$$

M is the total mass, N is the total number of particles, m_i is mass of atom i, $\boldsymbol{r}_i$ is the position of atom i, $\boldsymbol{r}_G$ is the position of center of gravity.

Here, R_g for all atoms was used. The result of R_g is shown in the Figure 3. In general, it changed from 0.6 nm to 0.75 nm, but temporarily increased to near 0.9 nm or decreased to near 0.5 nm.

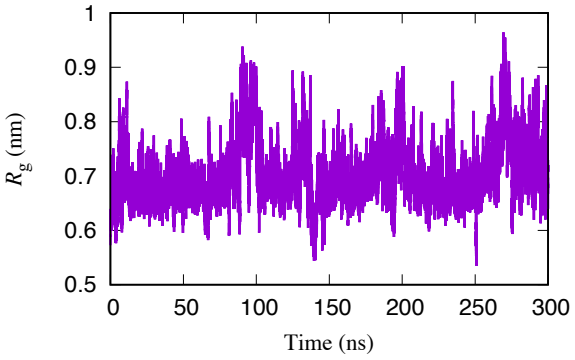

Figure 3. R_g for Chemerin-9.

3.1.3 Free Energy Landscape

It is known that proteins have various structures even with the same amino acid sequence. Over time, it is considered that the structure changes toward a stable structure with low free energy.

$$\Delta G = \Delta H - T\Delta S$$

ΔG is change of Gibbs energy, ΔH is change of enthalpy, T is temperature, and ΔS is change of entropy.

In this study, the free energy difference is calculated from the frequency distribution of the structure.

$$\Delta G(x, y) = -k_{\mathrm{B}} T \log \frac{P(x, y)}{P_{\max}}$$

$\Delta G(x, y)$ is Gibbs free energy, x and y are the reaction coordinates, k_{B} is Boltzmann constant, T is temperature, $P(x, y)$ is frequency distribution and $P_{\max}$ is maximum value of frequency distribution of structure.

In Figure 4, free energy topography is depicted with RMSD as x-axis and R_{g} as y-axis. Red indicates that the free energy is high, and the blue color indicates that the energy is low. The structure with the lowest energy was at 217.70 ns.

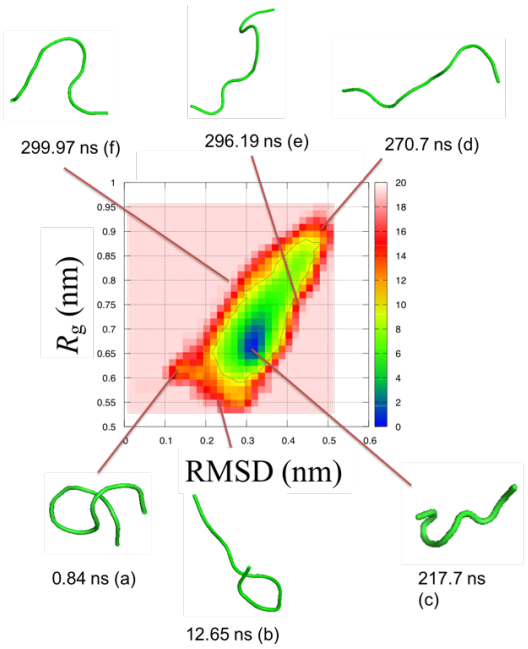

Figure 4. Free energy landscape for Chemerin-9.

3.1.4 RMSF

RMSF is a root mean square fluctuation, and is an index representing fluctuation from the initial state.

$$RMSF = \sqrt{\frac{1}{N_T}\sum_{i=1}^{N_T} |\boldsymbol{r}_i(t) - \langle \boldsymbol{r}_i \rangle|^2}$$

N_T is whole step of simulation, t is time, $r_i(t)$ is position of particle i at time t, $\langle \boldsymbol{r}_i \rangle$ is average position of particle i.

Here, the summation is for all peptide atoms. The results are shown in Figure 5. The fluctuation was large for amino acids with large side chains and amino acids with polarity, and the fluctuation was small for amino acids with small side chains.

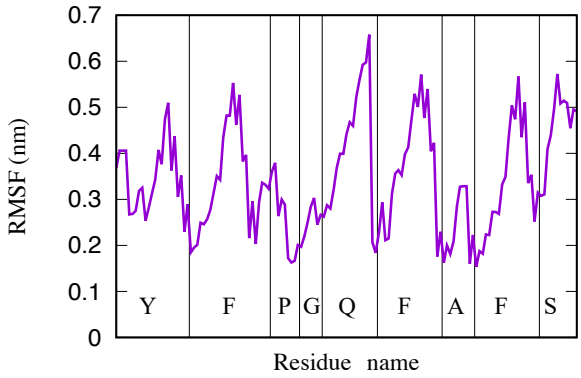

Figure 5. RMSF for Chemerin-9.

3.2 Docking Simulation

From the free energy topography of Chemerin-9 obtained by molecular dynamics simulation in the previous section, we extracted the six structures in Figure 4 and docked each with the ChemR23 receptor.

In this study, "affinity", defined in AutoDock Vina is used as a docking score to predict the binding affinity between Chemerin-9 and ChemR23 [14].

$$c = \sum_{i<j} f_{t_i t_j}(r_{ij})$$

c is "affinity", t_i is the type of atom i, r_{ij} is distance between atom i and atom j. $f_{t_i t_j}(r_{ij})$, interaction function of distance r_{ij}, is the sum of the energy of incentive interaction energy, repulsive energy, hydrogen bond energy, hydrophobic interaction energy, and energy proportional to the number of rotatable bonds [14].

We have performed docking simulation for the six structures shown in Figure 4.

The result of each docking simulation is shown in Table 1.

Table 1. Used model of chemerin-9 at x ns and affinity

Models	Affinity (kcal/mol)
0.84 ns (a)	-8.9
12.65 ns (b)	-9.1
217.70 ns (c)	-7.8
270.70 ns (d)	-7.8
296.19 ns (e)	-8.9
299.97 ns (f)	-8.9

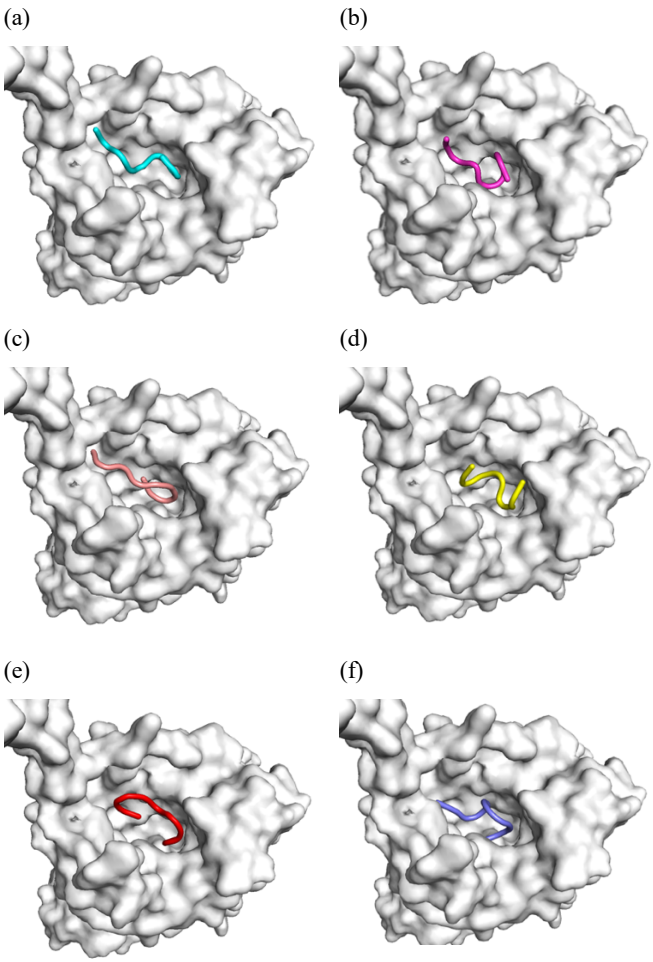

Figure 6. Docking models of Chemerin-9 and ChemR23.

3.3 Hydrogen Bonds

We investigate hydrogen bonds of docking models by using Pymol [15]. The largest number of hydrogen bonds is for models of 296.19 ns (e) and 299.97 ns (f) as shown in Table 2. The smallest number of hydrogen bonds is for model of 270.70 ns (d). Table 3 shows the residue numbers and amino acid types of the bound Chemerin-9 and ChemR23 receptors. Figure 7 shows the state of hydrogen bonding in the model (f) having the largest number of hydrogen bonds.

Table 2. The number of hydrogen bonds in docking models.

Models	The number of hydrogen bonds
0.84 ns (a)	5
12.65 ns (b)	5
217.70 ns (c)	5
270.70 ns (d)	4
296.19 ns (e)	6
299.97 ns (f)	6

Table 3. Residue number and amino acid type of Chemerin-9, ChemR23 receptor bound

Models	Chemerin9's residue number	ChemR23's residue number
0.84 ns (a)	9 (SER)	293 (SER)
	9 (SER)	30 (SER)
	9 (SER)	290 (SER)
	4 (GLY)	278 (ASN)
	4 (GLY)	274 (TYR)
12.65 ns (b)	1 (TYR)	101 (TYR)
	5 (GLN)	176 (ARG)
	7 (ALA)	278 (ASN)
	8 (PHE)	222 (ARG)
	9 (SER)	211 (GLY)
217.70 ns (c)	9 (SER)	209 (PRO)
	9 (SER)	209 (PRO)
	9 (SER)	212 (TYR)
	9 (SER)	211 (GLY)
	4 (GLY)	274 (TYR)
270.70 ns (d)	9 (SER)	37 (THR)
	7 (ALA)	101 (TYR)
	3 (PRO)	222 (ARG)
	1 (TYR)	300 (THR)
296.19 ns (e)	9 (SER)	215 (HIS)
	9 (SER)	274 (TYR)
	9 (SER)	222 (ARG)
	5 (GLN)	281 (GLU)
	8 (PHE)	176 (ARG)
	7 (ALA)	189 (ASN)
299.97 ns (f)	4 (GLY)	278 (ASN)
	1 (TYR)	101 (TYR)
	7 (ALA)	215 (HIS)
	9 (SER)	176 (ARG)
	9 (SER)	176 (ARG)
	9 (SER)	187 (CYS)

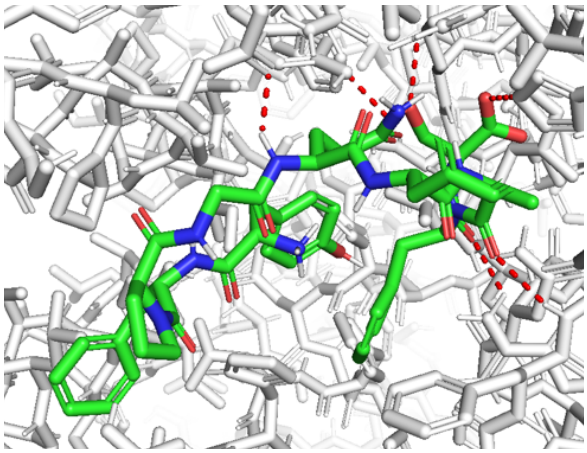

Figure 7. Hydrogen bonds for model (f). The red dashed line represents a hydrogen bond.

4. DISCUSSION and CONCLUSION

4.1 Molecular Dynamics Simulation

From the analysis of RMSD and R_g, it was found that Chemerin-9 has a large fluctuation when the structure is maintained. From the free energy topography, the simulation up to 300 ns showed that the structure at 217.70 ns had the lowest energy. From the results of RMSF analysis, it was found that fluctuations were large for amino acids with large side chains and amino acids with polarity, and fluctuations were small for amino acids with small side chains. A study of Chemerin-9 using alanine scan mutagenesis [6] states that the 1st Y, 2nd F, 4th G, 6th F, and 8th F amino acids are important for Chemerin-9 activity. These amino acids have large fluctuations except for the fourth. From this, it can be considered that the large fluctuation of amino acids is greatly related to the activity of Chemerin-9.

4.2 Docking Simulation

From the results of the docking simulation, the lowest affinity was -9.1 kcal/mol using the 12.65 ns model. On the other hand, the affinity was high at -7.8 kcal/mol using the models at 217.70 ns and 270.7 ns. The model at 217.70 ns is a model with low free energy, but the model at 270.70 ns is a model with high free energy. It seems that this peptide chain is spreading. From this, it is considered that a model having high free energy and a low R_g (a model in which the peptide chain is contracted) is likely to bind.

4.3 Hydrogen Bond

From the results of hydrogen bonding, the docking models with low affinity (a, b, e, f in Table 1) generally had more hydrogen bonds (Table 2). However, the model with the lowest affinity (b) did not result in the highest number of hydrogen bonds. This is considered to be due to other intermolecular forces. Also, compared with studies using alanine scan mutagenesis [6], the 9th residue, which has little effect on Chemerin-9 activity, is associated with the ChemR23 receptor in this docking simulation (Table 3). This is considered to be because 9th residue is an amino acid at the C-terminal of Chemerin-9, and easily binds to the receptor. There was no model in which all amino acids important for chemerin-9 activity were hydrogen-bonded to ChemR23 receptor.

4.4 Future Topics

We would like to compare the structural stability of each docking model in aqueous solution by conducting molecular dynamics simulations and to elucidate amino acids important for Chemerin-9 activity at the molecular level by examining the state of hydrogen bonding. In addition, we should investigate the mechanism that leads to the suppression of atherosclerosis at the molecular level by examining the structural changes of ChemR23. In addition, we hope to make clear a more accurate bond strength by calculating the bond free energy and search for a model with stronger bonding.

5. REFERENCES

[1] Hansson, G. K., and Libby, P. 2006. The immune response in atherosclerosis: a double-edged sword. *Nat. Rev. Immunol*. 6, 508-519.

[2] Sato, K., Yoshizawa, H. Seki, T., Shirai, R., Yamashita, T., Okano, T., Shibata, K., Wakamatsu, M. J., Mori, Y., Morita, T., Matsuyama, T. A., Ishibashi-Ueda, H., Hirano, T., and Watanabe, T. 2019. Chemerin-9, a potent agonist of chemerin receptor (ChemR23), prevents atherogenesis. *Clin. Sci. (Lond)*, in press.

[3] Duvic, M., Nagpal, S., Asano, A. T., and Chandraratna, R. A. 1997. Molecular mechanisms of tazarotene action in psoriasis. *J. Am. Acad. Dermatol.* 37, 18-24.

[4] Ernst, M. C., and Sinal, C. J. 2010. Chemerin: at the crossroads of inflammation and obesity. *Trends Endocrinol. Metab.* 21, 660-667.

[5] Shimamura, K., Matsuda, M., Miyamoto, Y., Seo, T., and Tokita, S. 2009. Identification of a stable chemerin analog with potent activity toward ChemR23. *Peptides.* 30, 1529-1538.

[6] Wittamer, V., Gregoire, F., Robberecht, P., Vassart, G., Communi, D., Parmentier, M. 2004. The C-terminal nonapeptide of mature chemerin activates the chemerin receptor with low nanomolar potency. *J. Biol. Chem*. 12, 9956-9962.

[7] Kostopoulos, C. G., Spiroglou, S. G., Varakis, J. N., Apostolakis, E., and Papadaki, H. H. 2014. Chemerin and CMKLR1 expression in human arteries and periadventitial fat: a possible role for local chemerin in atherosclerosis? *BMC Cardiovasc. Disord.* 14, 56.

[8] Reverchon, M., Rame, C., Bertoldo, M., and Dupont, J. 2014. Adipokines and the female reproductive tract. *Int. J. Endocrionol.* 232454.

[9] Herova, M., Schmid, M., Gemperle, C., and Hersberger, M. 2015. ChemR23, the receptor for chemerin and resolving E1, is expressed and functional on M1 but not on M2 macrophages. *J. Immunol.* 194, 2330-2337.

[10] Yang, J., Yan, R., Roy, A., Xu, D., Poisson, J., and Zhang, Y. 2015. The I-TASSER Suite: protein structure and function prediction. *Nat. Methods.* 12, 7-8.

[11] Abraham, M. J., Murtola, T., Schulz, R., Pall, S., Smith, J. C., Hess, B., Lindahl, E. 2015. GROMACS: High performance molecular simulations through multi-level parallelism from laptops to supercomputers. *SoftwareX.* 1-2, 19-25.

[12] Berendsen, H. J. C., Grigera, J. R., and Straatsma, T. P. 1987. The missing term in effective pair potentials. *J. Phys. Chem*. 91, 6269-6271.

[13] Lindorff-Larsen, K., Piana, S., Palmo, K., Maragakis, P., Klepeis, J. L., Dror, R. O., and Shaw, D. E. 2010. Improved side-chain torsion potentials for the Amber ff99SB protein force field. *Proteins*. 78, 1950-1958.

[14] Trott, O., and Olson, J. A. 2010. AutoDock Vina: improving the speed and accuracy of docking with a new scoring function, efficient optimization and multithreading. *J. Comput. Chem.* 31, 455-461.

[15] DeLano, W. L. 2002. Pymol: an open-source molecular graphics tool. CCP4 Newsletter on protein crystallography, 40, 82-92.